Gene 732 (2020) 144367

Contents lists available at ScienceDirect

Gene

journal homepage: www.elsevier.com/locate/gene

Research paper

Effects of telomerase overexpression in the model organism *Caenorhabditis elegans*

Melih Bayat[a], Robyn E. Tanny[b], Ye Wang[b], Carla Herden[a], Jens Daniel[c], Erik C. Andersen[b], Eva Liebau[c], Daniel E.J. Waschk[a,d,*]

[a] Institute of Human Genetics, University of Münster, Vesaliusweg 12-14, Münster 48149, Germany
[b] Department of Molecular Biosciences, Northwestern University, Evanston, IL 60208, USA
[c] Institute of Animal Physiology, Department of Molecular Physiology, University of Münster, Schlossplatz 8, Münster 48143, Germany
[d] GENETICA MÜNSTER – Praxis für Humangenetik, Center for Human Genetics, Grevener Straße 105, Münster 48159, Germany

1. Introduction

The telomerase reverse transcriptase (*TERT*; OMIM 187270) is the catalytic subunit of the enzyme telomerase, which counteracts the shortening of telomeres by *de novo* addition of repetitive nucleotide sequences at the end of eukaryotic chromosomes (Greider, 1996; Greider, 1998). Nevertheless, telomerase activity is usually not sufficient to prevent telomere shortening due to incomplete DNA replication in each cell division over time. It is assumed that this shortening contributes to cellular senescence and organismal aging by limiting the number of cell divisions (Collado et al., 2007).

In humans, mutations in *TERT* lead to a wide spectrum of clinical defects. The most severe form is the multisystem disorder dyskeratosis congenita (OMIM 613989), which is characterized by symptoms of premature aging and a predisposition to malignancy (Armanios et al., 2005; Armanios, 2009). On the other hand, activation of telomerase can be found in most human cancers (Kim et al., 1994). The important role of *TERT* for oncogenesis is further supported by the observation that *TERT* inhibition causes apoptosis of cancer cells *in vitro* (Zhang et al., 1999).

In animal models like zebrafish and mice, telomerase deficiency also leads to signs of premature aging and death (Henriques et al., 2013; Jaskelioff et al., 2011; Anchelin et al., 2013). Overexpression of *Tert* in mice caused an increased risk of cancer (Boccardi and Paolisso 2014) as well as neurological symptoms similar to an autism-like behaviour (Kim et al., 2016). Interestingly, *Tert* overexpression in mice engineered to resist cancer showed a significant extension of median lifespan and a reduction in age-related disorders (Tomás-Loba et al., 2008). The same effects have been observed when telomerase was expressed in adult mice using adeno-associated virus (AAV) vectors (Bernardes de Jesus et al., 2012). Transfection of *TERT* into normal human cells leads to an extension of the maximum number of cell divisions and lifespan *in vitro* (Bodnar et al., 1998). Telomerase activation has therefore been suggested to be a viable therapeutic strategy to delay the onset of cellular senescence, tissue dysfunction, and organismal decline in humans, although evidence of such roles for telomerase activation in humans is still scarce and controversial (Boccardi and Paolisso 2014).

The *C. elegans* homologue of *TERT* is encoded by the gene *trt-1* (Meier et al., 2006). Animals deficient in *trt-1* show a progressive decrease in telomere length as well as brood size and typically fail to reproduce after a few generations (Cheung et al., 2006). It is assumed that telomerase deficiency negatively affects lifespan in *C. elegans* as well, but the impact of telomerase overexpression has not been studied in this model organism yet. We created a *C. elegans* strain with increased *trt-1* activity to investigate the effects on its lifespan and fertility as well as telomere lengths. To accomplish this goal, a strain with a single-copy insertion of *trt-1* cDNA as well as the corresponding control strain without the target gene were generated based on an approach described previously (Frøkjaer-Jensen et al., 2008; Frøkjær-Jensen et al., 2012).

2. Materials and methods

2.1. Generation of plasmids

The target plasmid containing the *trt-1* ORF (Dharmacon/GE Healthcare, Clone Id DY3.4 ORF) was generated with NEBuilder HiFi

Abbreviations: AAV, adeno-associated virus; Bp, base pairs; *C. briggsae*, *Caenorhabditis briggsae*; cDNA, DNA complementary to RNA; *C. elegans*, *Caenorhabditis elegans*; CGC, Caenorhabditis Genetics Center; DNA, deoxyribonucleic acid; *E. coli*, *Escherichia coli*; LB, Luria-Bertani (medium); NGM, Nematode growth media; MosSCI, *Mos1*-mediated single-copy insertion; OMIM, Online Mendelian Inheritance in Man; ORf, open reading frame; PCR, polymerase chain reaction; RNA, ribonucleic acid; *TERT*, telomerase reverse transcriptase; *trt-1*, *Caenorhabditis elegans* homologue of *TERT*; *trt-1* os, *trt-1* overexpression strain; Unc, uncoordinated; UTR, untranslated region

* Corresponding author at: GENETICA MÜNSTER – Praxis für Humangenetik, Center for Human Genetics, Grevener Straße 105, Münster 48159, Germany.
E-mail address: Daniel.Waschk@uni-muenster.de (D.E.J. Waschk).

https://doi.org/10.1016/j.gene.2020.144367
Received 12 September 2019; Received in revised form 10 January 2020; Accepted 13 January 2020
Available online 16 January 2020
0378-1119/

DNA Assembly Cloning Kit (New England Biolabs) according to the manufacturer's instructions. The *trt-1* ORF was flanked by the promotor of *dpy-30* (Dharmacon/GE Healthcare, Clone Id ZK863.6 Promoter) and the 3′ untranslated region (UTR) of *tbb-2* (Addgene Id pCM1.36, gift from Geraldine Seydoux), which were reported to promote expression in all cell types and at all developmental stages, and cloned into destination vector pCFJ150 (Addgene Id pCFJ150 - pDESTttTi5605[R4-R3], gift from Erik Jorgensen). Destination vector pCFJ150 contains a *C. briggsae unc-119* rescue fragment and genomic regions flanking the *ttTi5605* locus to generate *Mos1*-mediated single copy insertions (MosSCI) (Frøkjaer-Jensen et al., 2008; Frøkjær-Jensen et al., 2012). DNA fragments with the desired elements were amplified from each donor plasmid by polymerase chain reaction (PCR) and contained overlapping sequences for each adjacent fragment. Adjacent fragments were then enzymatically assembled at the overlapping sequences. During the plasmid construction, att-sites from the donor plasmids between *trt-1* ORF and both *dpy-30* Promotor and *tbb-2* 3′ UTR were removed. The control plasmid was generated with Q5 Site-Directed Mutagenesis Kit (New England Biolabs) according to the manufacturer's instructions. One fragment of pCFJ150 was amplified by PCR and ligated at its ends. In total, 1704 nucleotides from the donor plasmid pCFJ150 were removed between both att sites to reduce the size of the plasmid for microinjection and eliminate the chloramphenicol resistance and *ccdB* genes, which otherwise would be integrated into the genome of the transgenic *C. elegans* control strain. Target and control plasmids were grown in One Shot TOP10 Chemically Competent *E. coli* (Thermo Fisher Scientific) under selection of ampicillin. Correct assemblies of the *trt-1* target plasmid and the control plasmid were verified by Sanger sequencing. Plasmid maps of the target and control plasmids can be found in Figs. 1 and 2.

2.2. Generation of transgenic C. Elegans strains

Transgenic strains were transformed by microinjection of target and control plasmids into the gonads of *unc-119* deficient EG6699 worms (provided by CGC, funded by NIH Office of Research Infrastructure Programs [P40 OD010440]), which showed an uncoordinated (Unc) phenotype to generate stable single-copy insertions at the *ttTi5605* locus on chromosome II as described in detail previously (Frøkjaer-Jensen et al., 2008; Frøkjær-Jensen et al., 2012). Briefly, mobilization of a *Mos1* transposon in EG6699 worms driven by the *Mos1* transposase from a co-injected helper plasmid (Addgene ID pCFJ601 - P*eft-3 Mos1* transposase, gift from Erik Jorgensen) generates a double-stranded break in non-coding DNA. The break is repaired by copying DNA from an extrachromosomal template of the *trt-1* target plasmid into the *ttTi5605* locus. The control strain was generated accordingly by injecting the control plasmid (Fig. 2). Successful transformation was assessed by rescue of the Unc phenotype in the F1 progeny. Homozygous insertions were identified by the absence of Unc progeny of singled hermaphrodites and verified by PCR analyses and Sanger sequencing. Both strains were subsequently outcrossed five times with heavily outcrossed *unc-119* deficient PS6038 worms (provided by CGC) and counter-checked for complete homozygous insertions with PCR and Sanger sequencing. Besides the additionally inserted copy of *trt-1,* both the *trt-1* overexpression strain (*trt-1* os) and the control strain also carry the normal genomic copies of *trt-1*.

2.3. Fertility and lifespan experiments

Worms were kept in an incubator at stable 20 °C. Scoring of phenotypes and counting of progeny was carried out at room temperature. At day 0, synchronized stage 4 larvae (F1 generation) were transferred to a 35 mm petri dish (one worm per dish) containing 4 ml NGM, a centered spot of 50 µl *E. coli* OP50 in lysogeny broth (LB) medium as food source, and a reppellant ring of 10 mg/ml palmitic acid in ethanol at the edges of the NGM to avoid escapes. During their reproductive phase, worms were transferred to a fresh petri dish every 48 h. Worms were scored every 48 h for survival and category of body movement. Worms were scored as dead if no head motion could be provoked by prodding with a platinum wire. Worms were censored if they disappeared, died by external impact or internal hatching of larvae, and if the petri dish became contaminated. Body movement was classified according to categories described previously (Herndon et al., 2002; Huang et al., 2004). The beginning of senescence was defined as cessation of sinusoidal body movement. Results of lifespan and senescence experiments were confirmed in two independent assays. To quantify the brood size, F2 larvae were counted at 16x magnification 24 h after transfer of parental worms to a new petri dish. Worms with a brood size smaller than 10 were classified as infertile.

2.4. Statistical analyses

The software IBM SPSS statistics version 25 was used for statistical analyses. Kaplan–Meier estimator was used for calculating the survival

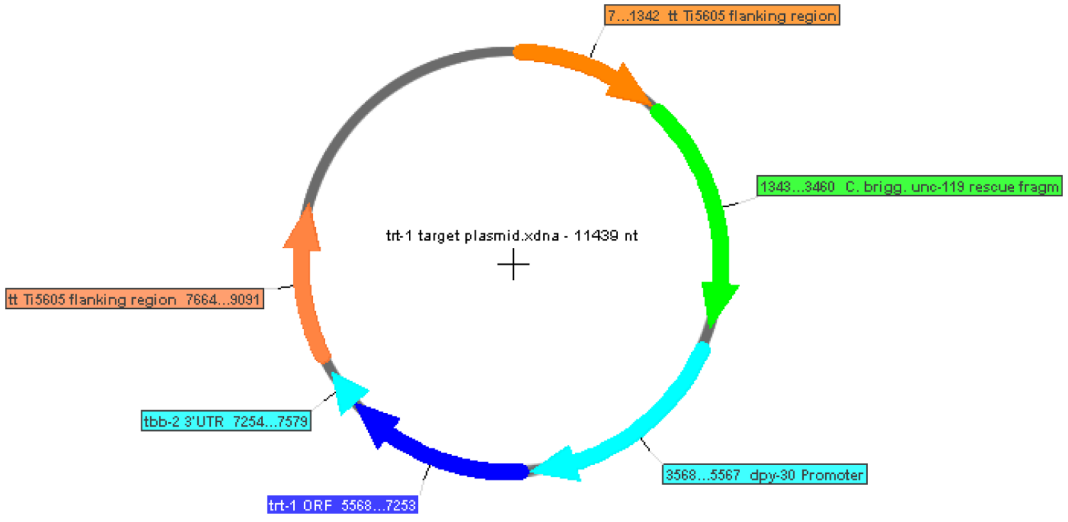

Fig. 1. Map of the *trt-1* target plasmid. The target plasmid containing the *trt-1* ORF was generated with NEBuilder HiFi DNA Assembly Cloning Kit according to the manufacturer's instructions. The *trt-1* ORF was flanked by the promotor of *dpy-30* and the 3′ untranslated region of *tbb-2* and cloned into destination vector pCFJ150. Destination vector pCFJ150 contains a *C. briggsae unc-119* rescue fragment and genomic regions flanking the *ttTi5605* locus to generate *Mos1*-mediated single copy insertions.

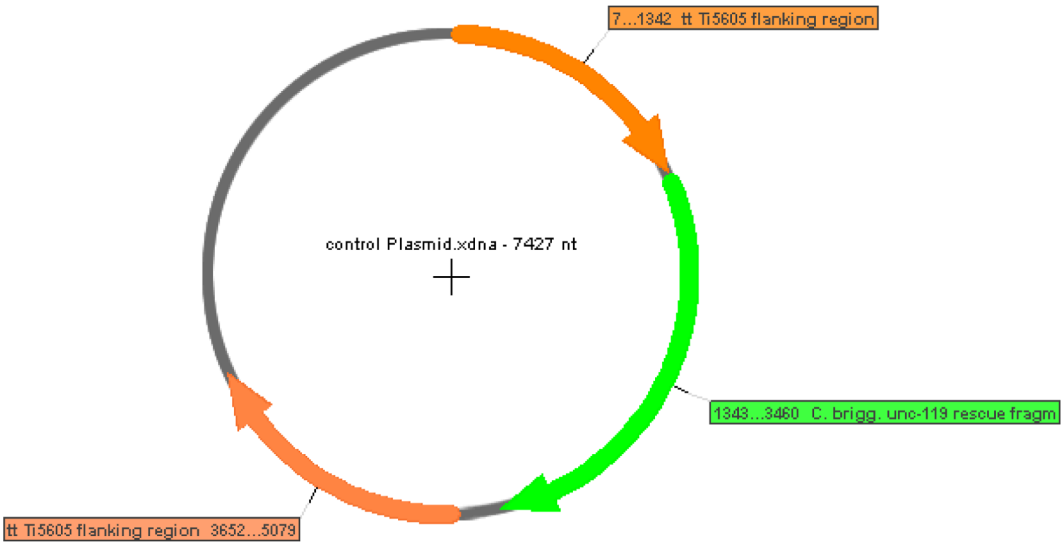

Fig. 2. Map of the control plasmid. The control plasmid was generated with Q5 Site-Directed Mutagenesis Kit according to the manufacturer's instructions. One fragment of destination vector pCFJ150 was amplified by PCR and ligated at its ends. Destination vector pCFJ150 contains a *C. briggsae unc-119* rescue fragment and genomic regions flanking the *ttTi5605* locus to generate *Mos1*-mediated single copy insertions.

of strains in days ± standard error. The Gaussian distribution of average brood size in number of larvae ± standard deviation was analysed using a Shapiro-Wilk test. The comparison of the average brood size was performed either with students *t*-test or Mann–Whitney *U* test. Worms that died or were censored until the end of day six were excluded from the analysis of average brood size. Values for $p < 0.05$ were considered statistically significant.

2.5. RNA expression analysis

Total RNA was isolated using the Monarch Total RNA Miniprep Kit (New England Biolabs) according to manufacturer's instructions. All samples were DNase I treated. First-strand cDNA was synthesized with the RevertAid First Strand cDNA Synthesis Kit (Thermo Scientific) using an oligo$(dT)_{18}$ primer at 42 °C for one hour. The following primers were used for subsequent quantitative real-time PCR of a 100 bp amplicon within exon 4 of *trt-1*:

Forward primer: 5′-TGTGGATCCAAATGTGAAGAGG-3′

Reverse primer: 5‘-CATAACTTGTCGTAAAGCC-3′

Primers were tested for specifity using NCBI BLAST and evaluated with MFOLD software in order to check for the formation of secondary structures at the site of primer binding. RNA analyses were run for the *trt-1* os, the transgenic control strain without the insert, the wild-type laboratory strain N2 (provided by CGC), and a no-template control. Quantitative RT-PCR was performed on a Light Cycler 480 (Roche) using the SensiMix SYBR Hi-ROX Kit (Bioline) according to the manufacturer's instructions. The cycling conditions were as follows: initial denaturation at 95 °C for 15 s, followed by 40 cycles of 15 s at 95 °C, 30 s at 60 °C, and 15 s at 72 °C. Following the final cycle, melting curve analysis was performed to verify the specificity in each reaction. Data analysis was performed with the software LightCycler 480 software version 1.5 (Roche). Expression pattern of the transgenic control strain without the insert was used as reference for the other samples. Differential gene expression was considered significant when the 95% confidence interval of the mean expression levels did not overlap.

2.6. Telomere-length analysis by sequencing

Telomere lengths were estimated using TelSeq (Ding et al., 2014) as described in the literature (Cook et al., 2016). In short, Illumina sequencing libraries were created using Nextera Sample Prep Kit and indexed using the Nextera Index kit as described previously (Andersen et al., 2015; Cook et al., 2016). Whole-genome sequencing was performed on an Illumina HiSeq4000. A Nextflow (Di Tommaso et al., 2017) pipeline identical to what was used in the analysis of *C. elegans* natural strain telomere lengths processed FASTQs into BAMs and then estimated telomere lengths. Strains were grown for ten generations before collecting genomic DNA to ensure that telomeres had stabilized their lengths. Telomere length estimation was performed in three assays for each strain.

3. Results

3.1. Lifespan and senescence

To analyze the impact of telomerase overexpression on the lifespan and senescene of *C. elegans*, we compared the results of the *trt-1* os with the transgenic control strain without the *trt-1* insert and the strain N2. Mean lifespan was 25.8 ± 1.6 days ($N = 30$) for the *trt-1* os, 21.0 ± 1.7 days ($N = 30$) for the transgenic control strain and 19.2 ± 2.2 days ($N = 30$) for the strain N2 (Fig. 3). The average lifespan was significantly higher in the *trt-1* os compared to the transgenic control strain (+22.9%, $p < 0.05$) as well as compared to the strain N2 (+34.4%, $p < 0.05$). The onset of senescence, which was defined as cessation of sinusoidal body movement, was delayed in the *trt-1* os as well. Mean onset of senescence was 18.6 ± 1.5 days for the *trt-1* os, 14.4 ± 1.2 days for the transgenic control strain, and 14.4 ± 1.7 days for the N2 strain (Fig. 3). In the *trt-1* os, the onset of senescence was delayed by 29.2% compared to the other strains.

3.2. Fertility

Fertility experiments were carried out for the *trt-1* os and the transgenic control strain without the *trt-1* insert at generations ten, twelve, and twenty, respectively (Fig. 4). At generation ten, the average brood size was 107.4 ± 75.8 ($N = 14$) in the *trt-1* os and 143.3 ± 48.5 ($N = 11$) in the transgenic control strain. The average brood size of the *trt-1* os was 25.1% lower compared to the control strain at generation ten ($p = 0.186$). Fertility decreased over time in the *trt-1* os to 20.9 ± 23.4 ($N = 14$) and 1.33 ± 2.4 ($N = 15$) at generation twelve and twenty, respectively. In the control strain, the brood size remained stable over time with values of 106.6 ± 26.6 ($N = 12$) and 159.9 ± 46.4 ($N = 19$) at generation twelve and twenty, respectively. Brood sizes were significantly lower in the *trt-1* os at

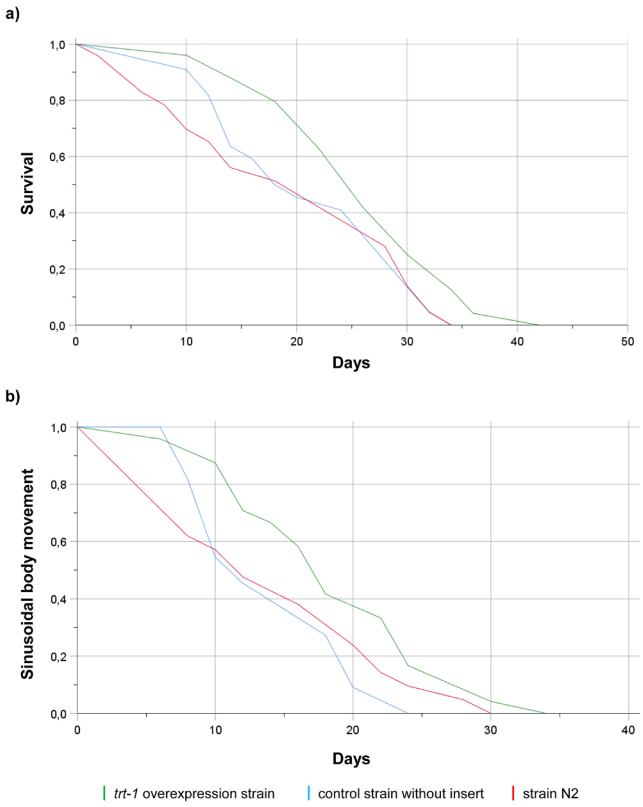

Fig. 3. Lifespan and senescence. (a) Mean lifespan was 25.8 ± 1.6 days for the *trt-1* overexpression strain, 21.0 ± 1.7 days for the transgenic control strain without the *trt-1* insert and 19.2 ± 2.2 days for the strain N2. The average lifespan was significantly higher in the *trt-1* overexpression strain compared to the transgenic control strain (+22.9%, $p < 0.05$) and also compared to the strain N2 (+34.4%, $p < 0.05$). (b) The onset of senescence was defined as cessation of sinusoidal body movement. Mean onset of senescence was 18.6 ± 1.5 days in the *trt-1* overexpression strain, 14.4 ± 1.2 days in the transgenic control strain without the *trt-1* insert and 14.4 ± 1.7 days in the strain N2. The onset of senescence was delayed in the *trt-1* overexpression strain by 29.2% compared to the control strain and the strain N2.

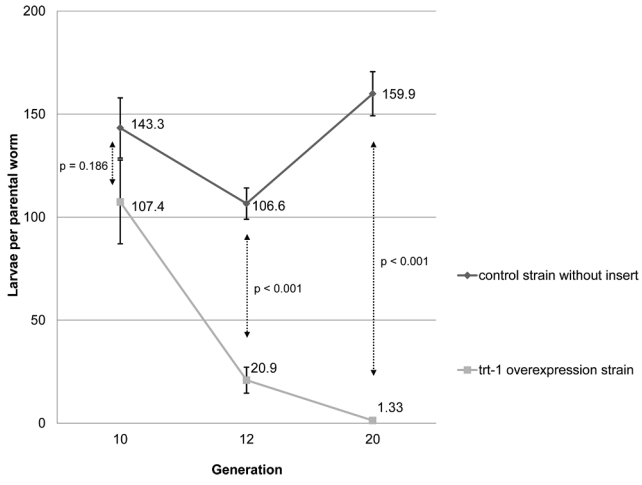

Fig. 4. Fertility. Average brood size dropped considerably within a few generations in the telomerase overexpression strain. Fertility was not reduced in the control strain without the *trt-1* insert over time. Fertility is shown as average number of larvae per parental worm.

generation twelve ($p < 0.001$) and twenty ($p < 0.001$). During the experiments, a growing fraction of infertile worms were also observed in the *trt-1* os with 14.3% at generation ten, 78.6% at generation twelve, and 93.3% at generation twenty (Fig. 5). There were no infertile worms in the control strain.

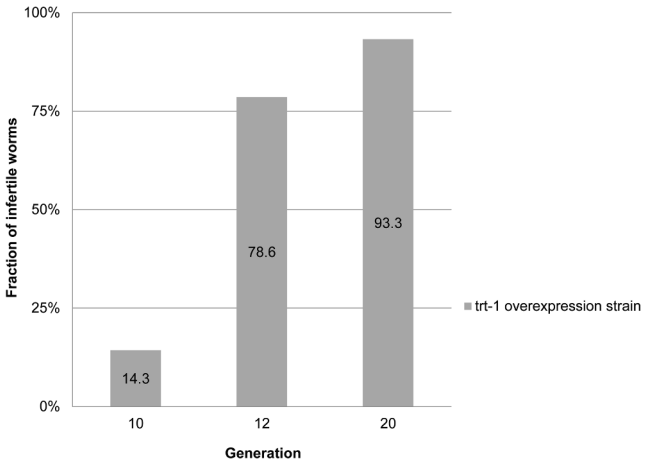

Fig. 5. Infertile worms. The fraction of infertile worms with a progeny of less than ten larvae increased rapidly in the *trt-1* overexpression strain. No infertile worms were observed in the control strain without the *trt-1* insert during the experiments.

3.3. RNA expression

RNA expression analysis was performed by quantitative real-time PCR of cDNA to evaluate the relative expression of *trt-1* in the *trt-1* os, the transgenic control strain without the insert, the strain N2, and a no-template negative control. The expression pattern of the transgenic control strain without the insert was used as reference for the other samples. Mean expression of *trt-1* in the transgenic control strain without the insert was 1.00 ± 0.37. Mean expression of *trt-1* was 357.50 ± 13.49 in the *trt-1* os and 10.56 ± 0.24 in the strain N2. No amplification was observed for the no-template negative control. Relative expression of *trt-1* was significantly higher in the *trt-1* os compared to the control strain without the insert ($p < 0.05$) and the N2 strain ($p < 0.05$).

3.4. Telomere-length analysis

To calculate the length of telomeres in the *trt-1* os and the control strain, we used a whole-genome sequencing technique that estimates the length of telomeres from counts of reads with hexameric repeats corresponding to *C. elegans* telomeres (Ding et al., 2014; Cook et al., 2016). Strains were grown for ten generations before collecting genomic DNA to ensure that telomeres have stabilized their lengths. We found that the control strain had longer telomeres (mean = 11.9 kb) than the *trt-1* overexpression strain (mean = 3.97 kb, difference $p = 0.0495$, Kruskal-Wallis rank sum test) (Fig. 6).

4. Discussion

4.1. Lifespan and senescence

Depending on the experimental design, an increase of lifespan from 9% to 26% has been observed in *Tert* overexpression mice (Tomás-Loba et al., 2008; Bernardes de Jesus et al., 2012). There are no reports about the effect of telomerase deficiency on lifespan of *C. elegans*, although unpublished data suggests that lifespan is reduced after *trt-1* knock-out (Han et al., 2006). In this study, lifespan was increased and the onset of senescence was delayed in the *trt-1* os. These findings support the hypothesis that lifespan can be extended and age dependent organismal decline delayed in multicellular organisms by artificially over-expressing telomerase. However, we did not observe longer telomeres

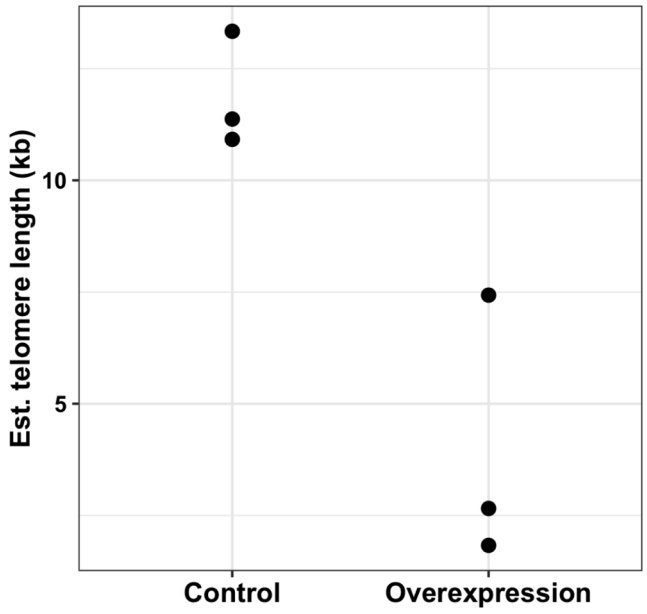

Fig. 6. Telomere length estimation. To calculate the length of telomeres in the *trt-1* overexpression strain and the control strain, we used a whole-genome sequencing technique that estimates the length of telomeres from counts of reads with hexameric repeats corresponding to *C. elegans* telomeres. Strains were grown for ten generations before collecting genomic DNA to ensure that telomeres have stabilized their lengths. Mean telomere length was longer in the control strain (11.9 kb) compared to the *trt-1* overexpression strain (3.97 kb, $p = 0.0495$).

in the telomerase overexpression strain. The importance of telomere lengths for the lifespan of *C. elegans* has been studied previously with contradictory results. An increase of lifespan after telomere elongation was found in a *C. elegans* strain with artificial overexpression of the telomere binding factor *hrp-1* (Joeng et al., 2004). On the other hand, no connection of telomere length and longevity could be observed in wild isolates of *C. elegans* (Raices et al., 2005; Cook et al., 2016). Taken this into account, mechanisms other than telomere elongation might be responsible for the lifespan extension and delayed senescence of the telomerase overexpression strain.

4.2. Fertility

A reduction of fertility as a consequence of telomerase deficiency has been reported for mice and zebrafish (Liu et al., 2002; Anchelin et al., 2013; Henriques et al., 2013). To our knowledge, there is no data available for the effect of telomerase overexpression on fertility of these models or other organisms. The average brood size of the telomerase overexpression strain in this study was significantly lower and showed a progressive decline over time compared to the transgenic control strain without telomerase overexpression. Furthermore, a growing fraction of infertile worms was observed in the *trt-1* os. In contrast to this, fertility remained stable in the control strain over time. A reduction of fertility has been observed in a *C. elegans* strain with a loss of function of *trt-1* (Cheung et al., 2006). We therefore expected the brood size of the *trt-1* os to be as high or higher compared to the control strain without telomerase overexpression before starting the experiments. However, the results suggest that fertility in *C. elegans* is highest at physiological levels of *trt-1* expression and that both reduction and increase of telomerase activity negatively affects fertility. A decrease of fertility in *trt-1* null mutants correlated with progressive shortening of telomeres (Cheung et al., 2006). In the present study a trend to shorter telomeres was observed in the telomerase overexpression strain in comparison to the control strain, suggesting that artificial telomerase overexpression could negatively affect telomere maintenance as well. Disruption of physiological telomere length homeostasis could therefore explain lower fertility by interfering with cell division and normal larval development in the *trt-1* os. In humans, the telomerase complex is built out of equimolar parts of telomerase reverse transcriptase (*TERT*; OMIM 187270), the telomerase RNA component (*TERC*; OMIM 602322) and the nucleolar protein dyskerin (*DKC1*; OMIM 300126) (Cohen et al., 2007). The telomerase complex associates with a holoenzyme protein, which is encoded by *WRAP53* (OMIM 612661) and which regulates telomerase trafficking (Venteicher et al., 2009). The overexpression of *TERT* alone might affect the correct stoichiometry of the telomerase complex or telomerase trafficking and hinder telomere synthesis. Furthermore, reduced fertility could be caused by a neomorphic effect of *trt-1* overexpression that is different from wild-type function of normal telomerase.

4.3. Summary

In this study, *trt-1* overexpression in *C. elegans* is associated with an extension of lifespan and a delayed onset of senescence. However, fertility was severely compromised and brood size further decreased over time. Moreover, a trend to shorter telomeres was observed in the telomerase overexpression strain, which might indicate a disruption of telomere maintenance and explain the reduction of fertility. These findings suggest that further investigation into the negative effects of artificial telomerase overexpression on fertility is required, especially before the application of telomerase activation in humans. Finally, it is important to note that if telomerase overexpression leads to a reduction of fertility only after several generations, this would be observed more rapidly in short-lived models like *C. elegans* compared to other organisms with longer generation times, including mice and humans.

CRediT authorship contribution statement

Melih Bayat: Investigation, Formal analysis, Writing - original draft. **Robyn E. Tanny:** Investigation, Writing - review & editing. **Ye Wang:** Investigation, Writing - review & editing. **Carla Herden:** Investigation, Formal analysis, Writing - original draft. **Jens Daniel:** Investigation, Writing - review & editing. **Erik C. Andersen:** Investigation, Writing - review & editing. **Eva Liebau:** Investigation, Writing - review & editing. **Daniel E.J. Waschk:** Conceptualization, Methodology, Investigation, Formal analysis, Data curation, Supervision, Project administration, Funding acquisition, Visualization, Writing - original draft, Writing - review & editing.

Declaration of Competing Interest

The authors declare that they have no known competing financial interests or personal relationships that could have appeared to influence the work reported in this paper.

Acknowledgements

We thank Anja Lechtermann for invaluable logistic assistance, Lea Fuchs and Ann-Christin Tewes for maintaining the worms in our absence, Ingo Kennerknecht and Albrecht Röpke for helpful advice and Peter Wieacker for supporting the project from the beginning.

Funding

This work was supported by Medizinische Fakultät Münster; and Innovative Medizinische Forschung an der Medizinischen Fakultät Münster [grant number WA221401].

References

Anchelin, M., Alcaraz-Pérez, F., Martínez, C.M., Bernabé-García, M., Mulero, V., et al., 2013. Premature aging in telomerase-deficient zebrafish. Dis. Model Mech. 6 (5), 1101–1112.

Andersen, E.C., Shimko, T.C., Crissman, J.R., Ghosh, R., Bloom, J.S., et al., 2015. A powerful new quantitative genetics platform, combining *Caenorhabditis elegans* high-throughput fitness asays with a large collection of recombinant strains. G3. (Bethesda) 5 (5), 911–920.

Armanios, M., Chen, J.L., Chang, Y.P., Brodsky, R.A., Hawkins, A., et al., 2005. Haploinsufficiency of telomerase reverse transcriptase leads to anticipation in autosomal dominant dyskeratosis congenita. Proc. Natl. Acad. Sci. U.S.A. 102 (44), 15960–15964.

Armanios, M., 2009. Syndromes of telomere shortening. Annu. Rev. Genom. Hum. Genet. 10, 45–61.

Bernardes de Jesus, B., Vera, E., Schneeberger, K., Tejera, A.M., Ayuso, E., et al., 2012. Telomerase gene therapy in adult and old mice delays aging and increases longevity without increasing cancer. EMBO Mol. Med. 4 (8), 691–704.

Boccardi, V., Paolisso, G., 2014. Telomerase activation: a potential key modulator for human healthspan and longevity. Ageing Res. Rev. 15, 1–5.

Bodnar, A.G., Ouellette, M., Frolkis, M., Holt, S.E., Chiu, C.P., et al., 1998. Extension of lifespan by introduction of telomerase into normal human cells. Science 279 (5349), 349–352.

Cheung, I., Schertzer, M., Rose, A., Lansdorp, P.M., 2006. High incidence of rapid telomere loss in telomerase-deficient *Caenorhabditis elegans*. Nucleic Acids Res. 34 (1), 96–103.

Cohen, S.B., Graham, M.E., Lovrecz, G.O., Bache, N., Robinson, P.J., et al., 2007. Protein composition of catalytically active human telomerase from immortal cells. Science 315 (5820), 1850–1853.

Collado, M., Blasco, M.A., Serrano, M., 2007. Cellular senescence in cancer and aging. Cell 130 (2), 223–233.

Cook, D.E., Zdraljevic, S., Tanny, R.E., Seo, B., Riccardi, D.D., et al., 2016. The genetic basis of natural variation in *Caenorhabditis elegans* telomere length. Genetics 204 (1), 371–383.

Ding, Z., Mangino, M., Aviv, A., Spector, T., Durbin, R., 2014. Estimating telomere length from whole genome sequence data. Nucl. Acids Res. 42, 1–4.

Di Tommaso, P., Chatzou, M., Floden, E.W., Barja, P.P., Palumbo, E., et al., 2017. Nextflow enables reproducible computational workflows. Nat. Biotechnol. 35 (4), 316–319.

Frøkjaer-Jensen, C., Davis, M.W., Hopkins, C.E., Newman, B.J., Thummel, J.M., et al., 2008. Single-copy insertion of transgenes in *Caenorhabditis elegans*. Nat. Genet. 40 (11), 1375–1383.

Frøkjær-Jensen, C., Davis, M.W., Ailion, M., Jorgensen, E.M., 2012. Improved Mos1-mediated transgenesis in *C. elegans*. Nat. Methods 9 (2), 117–118.

Greider, C.W., 1996. Telomere length regulation. Annu. Rev. Biochem. 65, 337–365.

Greider, C.W., 1998. Telomeres and senescence: the history, the experiment, the future. Curr. Biol. 8 (5), R178–R181.

Han, W.Y., B.K. Oh, Y.H. Shim, 2006 Haploinsufficiency of trt-1 in germ-line development of Caenorhabditis elegans [abstract]. In: East Asia C. elegans Meeting. 2006 Nov. 15-18, Seoul, Korea.

Henriques, C.M., Carneiro, M.C., Tenente, I.M., Jacinto, A., Ferreira, M.G., 2013. Telomerase is required for zebrafish lifespan. PLoS Genet. 9 (1) e1003214.

Herndon, L.A., Schmeissne, P.J., Dudaronek, J.M., Brown, P.A., Listner, K.M., et al., 2002. Stochastic and genetic factors influence tissue-specific decline in ageing *C. elegans*. Nature 419 (6909), 808–814.

Huang, C., Xiong, C., Kornfeld, K., 2004. Measurements of age-related changes of physiological processes that predict lifespan of *Caenorhabditis elegans*. Proc. Natl. Acad. Sci. U.S.A. 101 (21), 8084–8089.

Jaskelioff, M., Muller, F.L., Paik, J.H., Thomas, E., Jiang, S., et al., 2011. Telomerase reactivation reverses tissue degeneration in aged telomerase-deficient mice. Nature 469 (7328), 102–106.

Joeng, K.S., Song, E.J., Lee, K.J., Lee, J., 2004. Long lifespan in worms with long telomeric DNA. Nat. Genet. 36 (6), 607–611.

Kim, K.C., Rhee, J., Park, J.E., Lee, D.K., Choi, C.S., et al., 2016. Overexpression of telomerase reverse transcriptase induces autism-like excitatory phenotypes in mice. Mol. Neurobiol. 53 (10), 7312–7328.

Kim, N.W., Piatyszek, M.A., Prowse, K.R., Harley, C.B., West, M.D., et al., 1994. Specific association of human telomerase activity with immortal cells and cancer. Science 266 (5193), 2011–2015.

Liu, L., Blasco, M., Trimarchi, J., Keefe, D., 2002. An essential role for functional telomeres in mouse germ cells during fertilization and early development. Dev. Biol. 249 (1), 74–84.

Meier, B., Clejan, I., Liu, Y., Lowden, M., Gartner, A., et al., 2006. trt-1 is the *Caenorhabditis elegans* catalytic subunit of telomerase. PLoS Genet. 2 (2) e18.

Raices, M., Maruyama, H., Dillin, A., Karlseder, J., 2005. Uncoupling of longevity and telomere length in *C. elegans*. PLoS Genet. 1 (3) e30.

Tomás-Loba, A., Flores, I., Fernández-Marcos, P.J., Cayuela, M.L., Maraver, A., et al., 2008. Telomerase reverse transcriptase delays aging in cancer-resistant mice. Cell 135 (4), 609–622.

Venteicher, A.S., Abreu, E.B., Meng, Z., McCann, K.E., Terns, R.M., et al., 2009. A human telomerase holoenzyme protein required for Cajal body localization and telomere synthesis. Science 323 (5914), 644–648.

Zhang, X., Mar, V., Zhou, W., Harrington, L., Robinson, M.O., 1999. Telomere shortening and apoptosis in telomerase-inhibited human tumor cells. Genes Dev. 13 (18), 2388–2399.